Phosphoproteomic and Kinomic Signature of Clinically Aggressive Grade I (1.5) Meningiomas Reveals Rb1 signaling as a Novel Mediator and Biomarker

Carolina Angelica Parada[1], Joshua W. Osbun[1], Tina Busald[1], Yigit Karasozen[1], Sumanpreet Kaur[1], Min Shi[2], Jason Barber[1], Widya Adidharma[1], PJ Cimino[2], Catherine Pan[2], Luis Francisco Gonzales-Cuyar[2], Robert Rostomily[1], Don E. Born[2], Jing Zhang[2], Manuel Ferreira Jr.[1*]

[1]Departments of Neurosurgery/University of Washington School of Medicine, University of Washington Medical Center, Seattle/WA, 98195, USA

[2]Department of Pathology/University of Washington School of Medicine, Harborview Medical Center, Seattle/WA, 98104, USA

Running Title: Proteomic Genetic Aggressive meningiomas RB1 S780 biomarker

Keywords: meningioma, proteomics, phosphorylation, RB1, sequencing, phosphoproteomics, biomarker

Financial Support: University of Washington Department of Neurosurgery, Goertzen Foundation and Kapogiannatos family funds (M. Ferreira). The funding sources had no role in the design and conduct of the study, collection, management, analysis and interpretation of the data, preparation, review or approval of the manuscript, or decision to submit the manuscript for publication.

Declaration of Interests: The authors declare no competing interests.

*Corresponding Author

Manuel Ferreira Jr. MD, PhD

University of Washington Medical Center
1959 NE Pacific Street
Box 356470
Seattle, WA 98195-6470
206 543 3570 (o)
206 543 8315 (f)
manuelf3@uw.edu

Word Count: 6170

Total Number of Figures: 4

Total Number of Tables: 2

Supplemental Information: Figures 8 and Tables 12

Translational Relevance:

Cranial meningiomas are heterogeneous. WHO grade using histopathological criteria falls short in predicting progression free survival in some benign grade I tumors. Molecular diagnostics have become important in accurately grading other tumors of the brain, and thus better predicting the natural history. Using proteomic techniques in a group of genetically-defined clinically aggressive grade I meningiomas (grade 1.5 meningiomas; recurrent, progressive WHO grade I tumors requiring further treatment within 10 years), RB1 phosphorylation at the S780 site proved to be a biomarker and mediator of this group. While mutations in NF2, SMO, AKT, KLF4, TRAF7 or wild-type genotypes did not identify grade 1.5 meningiomas, RB1 phosphorylation at S780 defined the group. Utilizing a phosphoproteomic approach identified phosphorylation at S780 in RB1, a long-appreciated tumor suppressor gene. Validation of this biomarker in larger cohorts from independent medical centers is warranted. Further, additional molecular study may shed light onto how RB1 S780 is involved with the behavior of clinically aggressive grade 1.5 meningiomas.

Abstract

Purpose: Most WHO Grade I meningiomas carry a favorable prognosis. Some become clinically aggressive with recurrence, invasion, and resistance to conventional therapies (grade 1.5; recurrent/progressive WHO grade I tumors requiring further treatment within 10 years). We aimed to identify biomarker signatures in grade 1.5 meningiomas where histopathology and genetic evaluation has fallen short.

Experimental Design: MS-based phosphoproteomics and peptide chip array kinomics were used to compare grade I and 1.5 tumors. Ingenuity Pathway Analysis (IPA) identified alterations in signaling pathways with validation by western blot. The selected biomarker was evaluated in an independent cohort of 140 samples (79/140 genotyped for meningioma mutations) by tissue microarray and correlated with clinical variables.

Results: The MS-based phosphoproteomics revealed differential Ser/Thr phosphorylation in 32 phosphopeptides. The kinomic profiling by peptide chip array identified 10 phosphopeptides, including a 360% increase in phosphorylation of RB1, in the 1.5 group. IPA of the combined datasets and western blot validation revealed regulation of AKT and Cell Cycle Checkpoint cascades. Rb1 hyperphosphorylation at the S780 site distinguished grade 1.5 meningiomas in an independent cohort of 140 samples and was associated with decreased progression/recurrence-free survival. Mutations in *NF2, TRAF7, SMO, KLF4, and AKT1* E17K did not predict RB1 S780 staining or progression in grade 1.5 meningiomas.

Conclusions: Rb1 S780 staining distinguishes grade 1.5 meningiomas, independent of histology, subtype, WHO grade or genotype. This promising biomarker for risk stratification of histologically bland WHO grade I meningiomas provides insight into the pathways of oncogenesis driving these outlying clinically aggressive tumors.

Introduction

Meningiomas account for one-fourth of all primary brain neoplasms (1). The World Health Organization (WHO) provides a link between histopathology and risk of progression/recurrence by classifying meningiomas as grade I (benign), grade II (atypical, clear cell and chordoid subtypes), or grade III (anaplastic) (2). There are 9 different histological subtypes of WHO I, with the majority cured by surgery. Some WHO grade I tumors metastasize (3), rapidly grow (4), invade brain, blood vessels and cranial nerves (5). Benign meningiomas can reoccur after gross total resection (6) with rapid progression (7). Radiation or radiosurgery are reserved for when surgery is no longer an option, although some tumors prove refractory (8). These observations support the concept of a group of histologically benign meningiomas, which unexpectedly behave clinically aggressive.

WHO I meningiomas lack atypical or anaplastic features, and are managed as benign tumors. Brain invasion is enough to upgrade otherwise bland tumors to grade II (atypical), but is dependent on capturing brain tissue on the pathology section. These tumors have higher rates of recurrence, progression and altered mortality rates (9). Identification of these tumors is imperative for treatment.

Molecular markers are needed to identify clinically aggressive grade I meningiomas (grade 1.5 meningiomas; recurrent, progressive WHO grade I tumors requiring further treatment within 10 years (10)), where histology falls short. The grade 1.5 meningioma follows a more clinically aggressive natural history as compared to its WHO grade I counterpart. Deletion of 1p and/or 14q is thought to predict recurrence and progression, correlating with tumor grade (6, 11). Recent studies show that benign tumors with similar alterations in their genome can become clinically aggressive and reoccur (12). These results have not translated into biomarkers for diagnosis, risk stratification nor offer chemotherapeutic targets. Recently, methylation status was shown to segregate WHO I tumors, and lower risk WHO II meningiomas (13), suggesting that epigenetics may play a larger role.

Pathways in cancer cells lead to increased proliferation, differentiation, migration, and survival. Post-translational modifications include phosphorylation by kinases. Advances in proteomic techniques have led to a new understanding of the phosphoproteome in human tissue (14) and cell lines (15). Peptide arrays (16), reverse-phase protein arrays (17), antibody arrays (18) and mass spectrometry (MS; 16) have been used to characterize cancer. Phosphoproteomics have resulted in advances in

oncology; phosphorylation of oncoproteins in their native environment, molecular mechanisms that drive tumorigenesis (17), radio-resistance (19), cellular networks of drug response (20). From these data, pharmacological targets have led to the development of kinase inhibitors.

Few studies have investigated the proteome of benign meningiomas (21, 22). Most of them lack clinical information and compare different grades. Our group used phosphoproteomics to establish signatures of histologically well-defined WHO grade I-III meningiomas (16). Using low-resolution 2D gel followed by MS identification we also described unique proteins in clinically aggressive WHO I meningiomas (10). Utilizing higher-resolution phosphoproteomics we aimed to further characterize grade 1.5 meningiomas for risk stratification and evaluation of patterns of oncogenesis.

Methods

Tissue specimens, patients and clinical data

Studies were conducted in accordance with U.S. Common Rule ethical guidelines. Data and specimen collection were reviewed and approved by the University of Washington Institutional Review Board and Human Subjects Division. Written informed consent was obtained from all subjects. Methods were carried out in accordance with relevant guidelines and regulations. Patients underwent surgery at the University of Washington Hospitals between January 1st 1998 and December 31st 2012. Samples were collected and stored in -80^{o}C. Data was gathered regarding history, demographics, imaging, neuropathology reports, operative information, and outcomes. Resected tumors were re-graded according to revised criteria (2). Histological subtype, mitoses, Ki-67/MIB, sheeting, macronuclei, hypercellularity, and necrosis were recorded. Invasion was recorded from operative or pathology reads. Specimens were reviewed by three neuropathologists and neurosurgeons. Total resection was defined as absence of residual enhancement on post-operative MRI within 48 hours of surgery. Recurrence was defined as at least 1cm of enhancement on subsequent MRI. Progression was considered to be at least 1cm of growth of residual tumor on MRI after surgery. Patients were initially divided according to tumor grade (WHO I, II and III). Benign meningiomas were grouped into: clinically “non-aggressive” WHO grade I meningioma, designated as WHO I and clinically “aggressive” WHO grade I meningioma designated as grade 1.5. WHO I meningiomas underwent complete resection, with no evidence of progression/recurrence on imaging at a follow-up period of 120 months. Grade 1.5 included: 1) Patients undergoing gross resection for a WHO I meningioma requiring repeated resection for recurrence within 120 months (second surgery confirming WHO I), 2) Patients undergoing gross resection of a WHO I meningioma and requiring Stereotactic Radiosurgery (SRS) for a recurrence within 120 months, and demonstrating progression despite SRS. 3) Patients undergoing more than two operations for a recurrent WHO I tumor. The discovery set included five individual meningioma fresh-frozen tissue samples classified as WHO I, and five classified as grade 1.5. Clinical and histological features of the discovery set are described in Supplementary Table S1 and Table S2, respectively. The Cohort 01 tissue microarray (TMA) included 81 meningioma samples (31 grade I, 19 grade 1.5, 27 grade II, and 4 grade III) (Supplementary Table S3). Five samples (sample ID 2, sample ID 24, sample ID 46, sample ID 51, and sample ID 76) were excluded from the analysis due to tissue loss during sectioning, transfer, or

staining. The values of staining obtained for the sample ID 13 and 14 were averaged since they are from the same patient and resected at same surgery. Cohort 02 included target resequencing of *NF2, TRAF7, SMO, KLF4, and AKT1* E17K of 20 tumors (from Cohort 01, Supplementary Table S3). Target resequencing was performed in 59 additional cases in Cohort 03, and stained for RB1 S780 in this TMA (Supplementary Table S4).

Targeted resequencing with Molecular Inversion Probes (MIP)

DNA was extracted using QIAamp DNA Mini Kit (Qiagen, Valencia, CA) following quantification on Qubit (Life Technologies, Foster City, CA, USA). Probes were synthesized by Integrated DNA Technologies, Inc. (Redwood City, CA), pooled and phosphorylated. Sequencing and analysis were performed as described (16). Reads were mapped to GRCh37 using BWA-MEM after the MIP targeting sequence was hard clipped from the read. Indel realignment and base quality recalibration was performed according to GATK Best Practice's documentation. Variants were called using GATK's HaplotypeCaller in gvcf format and subsequently jointly called using GATK's GenotypeGVCF. A cut-off allele frequency > 4% was applied.

iTRAQ labeling and phosphopeptide enrichment

We utilized techniques similar to our prior work (16). Briefly, proteins were extracted from fresh-frozen meningioma specimens with T-PER Buffer (Thermo Scientific Pierce, Pittsburgh, PA) supplemented with 1:100 Phosphatase Inhibitor Cocktail and 1:100 Halt Protease Inhibitor Cocktail EDTA free (Thermo Scientific Pierce, Pittsburgh, PA). Protein lysates were quantified by Quibit. For the Isobaric Tags for Relative and Absolute Quantitation (iTRAQ)-based quantitative phosphoproteomic experiment, equal amounts of protein from five non-irradiated individual samples of WHO I and five non-irradiated individual samples from grade 1.5 meningioma were pooled to create two pools. Pooled lysates were precipitated, digested, labeled with tags (Life Technologies, Grand Island, NY); WHO I – iTRAQ114, and grade 1.5 – iTRAQ115, combined, and desalted. Phosphopeptides were allowed to bind to TiO_2 spin tips using Phosphopeptide Enrichment and Clean-up Kit (Thermo Scientific Pierce, Pittsburgh, PA), eluted, and cleaned using graphite columns (Thermo Scientific Pierce, Pittsburgh, PA). Samples were dried and resuspended in TFA. LC MS/MS analysis was performed as described previously (16). The spotted sample plates were analyzed using 4800 Plus MALDI

TOF/TOF TM (AB SCIEX, Framingham, MA) with mass range of 800–3500 m/z and S/N >50. MS/MS spectral data were analyzed using ProteinPilot 4.0 (AB SCIEX, Framingham, MA) referencing International Protein Index (IPI) and UniProtKB/Swiss-Prot database using Proteome Discoverer 1.3 (Thermo Scientific, Pittsburgh, PA) with the parameters: MMTS for cysteine alkylation, up to two trypsin missed cleavages; biological modification, amino acid and substitutions were set for ID focus; phosphorylation emphasis, FDR <5%, and confidence >95%. Data were normalized, and quantification expressed as ratio with WHO I levels (iTRAQ 114) as the denominator. A protein was considered differentially expressed when the iTRAQ ratio (grade 1.5:WHO I) was >1.20 or <0.83, or a fold change >20%. The fold-change cutoff for up- or down-regulation was determined based on pilot studies evaluating the label-specific experimental variation between two replicates for the same experimental group. Similar approaches have been employed by our group (16, 23, 24, 25) and others (26, 27) to identify relevant candidates in iTRAQ studies.

Serine/threonine kinase (STK) profiling

The PamStation®12 and STK PamChip® peptide array (PamGene International BV, Hertogenbosch, Netherlands) were used (16). The fluorescent platform measures the ability of active kinases in a specimen to phosphorylate specific peptides imprinted on multiplex chip arrays. Each chip contains 4 arrays. Each array displays 140 Ser/Thr and 4 positive control immobilized peptides. Each peptide represents a 15 amino-acid sequence from putative phosphorylation sites in human proteins derived from the literature and correlated with one or multiple upstream kinases. Kinase(s) in the sample actively phosphorylate substrates on the PamChip®, in the presence of ATP. An antibody is used to detect phosphorylation, and a 2nd FITC-conjugated antibody is used to quantify the signal. Three temperature-controlled peptide chips ran in parallel. Chips were blocked with 2% BSA (Sigma-aldrich, St. Louis, MO)**.** Proteins were extracted from fresh-frozen meningiomas with T-PER Buffer (Thermo Scientific Pierce, Pittsburgh, PA) supplemented with 1:100 Phosphatase Inhibitor Cocktail and 1:100 Halt Protease Inhibitor Cocktail EDTA free (Thermo Scientific Pierce, Pittsburgh, PA). Protein lysates were quantified by Quibit. Equal amounts of protein from five non-irradiated individual samples of WHO I and five non-irradiated individual samples from grade 1.5 meningiomas were pooled to create two pools (WHO I and 1.5). 1 µg of protein from each pool was applied to individual arrays with kinase buffer, 400 µM ATP, and FITC-

conjugated antibodies. Signal intensities were quantitated by BioNavigator 6.1.42 (PamGene), expressed per 100 ms exposure and log transformed. Mean value <20% for peptides with a signal >2000 was considered to ensure quality standards. Normalization was applied. Three replicated quantitations were combined using FDR <1%. A p-value <0.05 and a >10% fold change, were considered significant.

Western blot analysis

Three WHO I (1174, 1289, 1149) and three grade 1.5 samples (1432, 1494, 1893), which were part of our discovery set (Table S1, and S2), were submitted to western blot for validation. The other samples (WHO I: 1480, 6, and grade 1.5: 2002, 1379) were not included as these tissues were exhausted in performing MIP, iTRAQ mass spectrometry, and STK profiling. Proteins were extracted from meningioma fresh-frozen tissue with T-PER Buffer (Thermo Scientific Pierce, Pittsburgh, PA) supplemented with 1:100 Phosphatase Inhibitor Cocktail and 1:100 Halt Protease Inhibitor Cocktail EDTA free (Thermo Scientific Pierce, Pittsburgh, PA). Proteins were quantified using Quibit. 20ug of protein extract was combined with reducing Laemmli buffer, boiled for 5 min and then resolved by polyacrylamide gels. Polyacrylamide gels were transferred to PVDF membranes, incubated with primary antibody, overnight, and then with HRP-conjugated secondary antibody. Membranes were developed with Clarity Western ECL Substrate (Bio-rad, Hercules, CA) and visualized in GelDoc XR+ System (Bio-rad, Hercules, CA). For loading control, membranes were stripped and re-probed with anti-β-actin. Band intensity was quantified using Image Studio Lite Version 5.0 (LI-COR Biosciences, Lincoln, NE). Relative band densitometry is presented as mean ± SEM of the three samples of each meningioma grade. Antibodies are listed in Supplementary Table S5.

Tissue Microarray (TMA)

Samples were fixed in formalin, processed in tissue processor, and embedded in paraffin to produce FFPE blocks. Regions suitable for TMA were selected in duplicate. A blinded scientist created a randomized tissue microarray. All TMA slides for cohorts 01 and 03 were sectioned producing 4µm sections, placed on slides, and stained with H&E. Antibody optimization was performed using Leica Bond III Fully Automated IHC and ISH Staining System (Leica Bio-Systems, Buffalo Grove, IL). Anti-phospho-Rb1 S780 was used. The final step included the Bond Polymer Define Detection System (Leica Bio-Systems, Buffalo Grove, IL), containing endogenous peroxidase blocking, secondary

antibody, and a streptavidin–biotin detection system. Slides were counterstained with Gill's Hematoxylin. Controls were included with antibody run. The slides were scanned using NanoZoomer Digital Pathology System (Hamamatsu Photonics, K. K., San Jose, CA). Images were analyzed by Visiopharm (Hoersholm, Denmark) which converted the initial digital imaging into grayscale values using HDAB – DAB with the Chromaticity Red feature subtracted, an H&E with filter of 3X3 pixels, and an RGB - G feature. Analyses were conducted in a blinded fashion. Quantification of Rb1 was performed by automated image analysis of regions of interest. The ratio of Rb1 S780 per total tissue area was determined. The patterns of staining were divided into quartile groups (0, low, medium and high) and only the highest group used as high. The most stringent of criteria for labeling Rb1 as high was used and this objective cutoff was 0.088. Rb1 staining was considered low when ratio < 0.088 and considered high when ratio > 0.088.

Bioinformatics tools

Computational prediction of kinase phosphorylation was performed by GPS 2.1 (28) and PhosphoNet Kinexus (www.phosphonet.ca). Kinome trees were annotated using Kinome Render (29). Prediction of phosphorylation consensus motifs was performed by NetPhos server (30). IPA (Ingenuity Systems, Redwood City, CA) was used to identify mechanisms, functions, and predict upstream regulators. See reference 16.

Statistics

Comparison of the levels of the peptides/proteins in meningioma groups was performed using the nonparametric Mann-Whitney test and Kruskal-Wallis, when appropriate. Statistical significance of Rb1 S780 phosphorylation by grade was analyzed by mixed-effects regression using grade ranks to test for an ordinal relationship. Correlation between Rb1 S780 phosphorylation and clinical variables was assessed by Spearman and Kruskal-Wallis, as appropriate. Mutation prevalence by meningioma grade were evaluated using exact logistic regression. Analyses were adjusted for multiple comparisons using Holm-Bonferroni when appropriate. Time-to-recurrence was evaluated using log-rank tests and Cox regression. For the statistical analyses of band densitometry for Western Blotting, the data is presented as mean ± SEM of the three samples of each meningioma grade (P-values were calculated using both Student's t test and nonparametric testing. All differences were significant when $p < 0.05$.

Data Availability

Datasets generated and analyzed are available from the corresponding author on request.

Results

MS-based phosphoproteomic profiling of meningioma grade 1.5.

While alterations in *SMO*, *KLF4*, *TRAF7*, *NF2*, and *AKT* E17K have been found in meningiomas, the downstream protein signature underlying clinically aggressive WHO grade I meningiomas is unknown. In an attempt to understand protein specific alterations underlying a clinically aggressive phenotype of WHO grade I meningioma we utilized proteomic profiling. Phosphorylation and kinase activity could lead to novel mechanistic insight and potential biomarker identification and thus iTRAQ phosphopeptide enrichment followed by quantitative mass spectrometry analysis of the ten meningioma specimens (discovery set, Supplementary Table S1 and S2) was performed. WHO grade I and grade 1.5 pools were labeled iTRAQ114 and iTRAQ115, respectively, following mass spectrometry analysis (Supplementary Figure S1a). A total of 649 unique phosphopeptides corresponding to 165 proteins were identified (Supplementary Table S6). From the 649 candidates, we selected 32 unique phosphopeptides with an individual composite score of ≥95% confidence, top-ranked matching sequence for that spectrum, and iTRAQ ratios from meningioma grade 1.5 compared to benign WHO I tissue greater than 1.20 or less than 0.83 (fold change>20%) at a FDR<5% (Supplementary Figure S1b). Fifteen proteins (46.9%, n=15/32) showed hyperphosphorylation at Ser/Thr residues, among them the ABCF1, ABLIM1, ADD1, AKAP12, CTTN, PBDC1, DBNL, EIF4B, GLCE, HNRNPD, HSPB1, LMNA, Septin-2, VCAN, and VCL. Seventeen proteins (53.1%, n=17/32) showed hypophosphorylation at serine or threonine residues, including; ADD3, CANX, DPYSL3, EML4, EPB41L2, G3BP1, HSP90AB1, MAP1B, MARCKS, PGRMC1, PLEC, PPP1R2, SDC2, SEC22B, TGOLN2, TP53I1, and VIM. Western blot validation of the iTRAQ analysis was performed (Supplementary Figure S1c). Phosphoproteins for western blot validation were selected according to antibody commercial availability. The levels of phosphorylation or protein expression were analyzed in three individual fresh frozen tissue specimens of each meningioma grade, which were also part of the discovery set. We observed that phosphorylation of DPYSL3 S522 ($p = 0.003$), G3BP1 S232 ($p =$

0.004), and CANX S583 (p = 0.006) correlated with the phosphoproteome dataset (Supplementary Figure S1c, Supplementary Figure S2).

We used IPA to explore alterations in phosphorylation of 32 phosphoproteins (Supplementary Figures S3 and S4). PKC, cAMP/PKA, PI3K-MTOR-AKT, MAPK-ERK, and RHO GTPases are common themes in these cascades. The MKNK1 and mTOR were predicted as upstream regulators of the cascade (Supplementary Figure S4b).

Serine-Threonine kinome profiling of grade 1.5 meningiomas

We performed kinome profiling of WHO grade I and grade 1.5 meningiomas. Pooled lysates from fresh-frozen specimens were characterized using PamChip® peptide array Ser/Thr kinase platform (STK). The experimental workflow is shown in Figure 1a. Only peptides above the limit of detection were included (n=101/140) (Supplementary Table S7). The 2Log transformed signal intensities of the 101 peptides above limit of detection were clustered and represented as a heat map (Figure 1b, Supplementary Table S7). Fold change analysis of grade 1.5 versus WHO I meningiomas showed 10/101 peptides with significantly increased phosphorylation changes, among them RB_774_786. Rb1 demonstrated over a 360% increase in phosphorylation levels in the more clinically aggressive, 1.5 group (Figure 1c). This phospho-peptide contains three phospho-sites (T774, T778, and S780). Further, analysis of the phosphorylation consensus motif indicates that S780 in the motif T-R-P-P-T-L-S-P-I-P-H-I-P of Rb1 is the predicted phosphorylation site. This is a consensus site for CDKs kinases (Supplementary Figure S5c). Downstream activation of related signaling pathways (Figure 1d) was predicted in this group of tumors.

Combined analysis of the iTRAQ/MS-based global phosphoproteome and kinome for interpretation of signaling networks in grade 1.5 meningiomas.

We combined datasets (significantly altered 32 phosphopeptides in the iTRAQ and 10 proteins from the STK chip) to perform computational analysis, to gain insight into the mechanisms of grade 1.5 meningiomas. First, we utilized computational prediction of phosphorylation sites by their cognate Ser/Thr kinases. The analysis predicted 85 potential upstream kinase regulators mainly included in the AGC and CMGC groups (Supplementary Figure S3a). CDKs, CDC42, and MAPKs are three of the largest CMGC groups and mediate the function of a variety of tumor suppressors in the ERK-MAPK transduction pathway (32). The AGC group includes AKT, PKA, PKG, and PKC protein

kinases (33). The IPA analysis predicted mTOR as a regulator of grade 1.5 meningiomas (Supplementary Table S8, mTOR highlighted in yellow) and showed a direct relationship with hyperphosphorylated Rb1 as well as with FRAP1-Hd, SEC22B, HSPB1, G3BP1, SEPT2, PGRMC1, and HSP90AB1 (Supplementary Figure S5b). The Rb1 S780 site is a consensus site for CDKs kinases. Taken together, the computational analyses suggest that PI3K-AKT-mTOR, ERK-MAPK, PKA, CDC42-RAC1-RHOA, and Rb1/E2F signaling pathways may be altered in grade 1.5 meningiomas.

Canonical pathways and upstream kinases validation by Western Blotting

Western blot analysis of PI3K-AKT-MTOR, ERK-MAPK, PKA, CDC42-RAC1-RHOA, and Rb1/E2F signaling pathways (Figure 2 and Supplementary Figure S7) was performed. Significant decreases in AKT S473, AKT T308 and downstream targets IKKα T23, and RAF1 were found (PI3K-AKT-MTOR) (Figure 2a and Supplementary Figure S7a). In the ERK-MAPK pathway, the increased expression of p38 MAPK distinguishes the 1.5 group (Figure 2b and Supplementary Figure S7b). Phosphorylated cAMP/PKA targets, CAMKII and PKAC were seen (Figure 2c). Proteins intimately involved with the CDC42-RAC1-RHOA pathway played a smaller role and were not significantly altered in the grade 1.5 group of tumors (Figure 2d). Significantly increased levels of CDK4, CDK6 and Rb1 S780 were seen (Figure 2e and Supplementary Figure S7e), together implying a defining signature of cell cycle G1/S checkpoint signaling in grade 1.5 meningiomas**.** Figure 2f is a table illustrating significantly altered proteins and respective p values.

Hyperphosphorylation of Rb1 S780 predicts recurrence in WHO I meningiomas, identifying the 1.5 subgroup.

We used TMA methods to explore whether Rb1 S780 staining was found in meningiomas of varying grades, specifically grade 1.5 tumors. Rb1 S780 staining was analyzed in multiple TMA cohorts (Supplementary Table S9) which included samples prior to and after radiation treatment (Supplementary Table S10). The levels of Rb1 S780 staining were quantified (Supplementary Figure S8). Meningioma specimens with no prior radiation treatment (107 total tumors; 47 grade I, 28 grade 1.5, 31 grade II, and 1 grade III) and specimens with prior radiation treatment (33 total tumors; 0 grade I, 16 grade 1.5, 14 grade II, and 3 grade III) (Supplementary Table S3 and S4) were included. We performed univariate and multivariate analyses of Rb1 S780 phosphorylation to evaluate the ability to distinguish 1.5 tumors (Supplementary Table S11 and Table 3a).

Potential confounders revealed by the univariate analysis (Supplementary Table S11) were considered in the multivariate model (Table 1a). Rb1 S780 phosphorylation distinguishes 1.5 tumors. Rb1 S780 phosphorylation by grade is statistically significant and it is increased in grade 1.5 tumors in all samples (Figure 3c) as well as in samples with no prior radiation treatment (Figure 3d, Table 1a). Irradiated samples did not show differences in Rb1 S780 phosphorylation (Figure 3e, Table 1a). It is noteworthy that the discovery set of tumors were non-irradiated samples.

Kaplan Meier and Cox analyses of Rb1 S780 phosphorylation versus progression/recurrence-free survival were performed to identify its potential prognostic value. In all samples, independent of WHO grade, Rb1 S780 phosphorylation is associated with lower progression/recurrence-free survival ($p = 0.004$, Figure 3f, Table 1b). In non-irradiated samples ($p = 0.0001$) (Figure 3g, Table 1b) increased Rb1 S780 staining was also associated with decreased progression/recurrence-free survival. This was not visualized in the sample cohort with prior radiation treatment (Figure 3h, Table 1b).

Within the histologically benign samples, grade 1.5 meningiomas, had higher levels of phosphorylation of Rb1 at S780. Prior radiation tended to correlate with decreased phosphorylated Rb1 across groups (Figure 3e). Considering that radiation may change the characteristics of a tumor and only non-irradiated samples were present in the discovery set, we focused on the significance of progression/recurrence-free survival versus Rb1 S780 staining in samples without previous radiation, by grade. Phosphorylation of Rb1 at S780 in non-irradiated, histologically benign, tumors correlated with progression/recurrence-free survival (Figure 3j, Table 1b). This correlation was not seen in this group when radiation was given prior to the surgery (Figure 3k).

To better understand the role that Rb1 S780 staining plays in temporal aggressiveness of the grade 1.5 group of tumors we separated these tumors based on the timing of the sample collection. That is, whether the sample was obtained at the first operation versus the 2^{nd}-5^{th} surgery in the patient's course of treatment. There were 140 meningiomas stained for Rb1 S780 (of which 79 underwent MIP resequencing). This included 47 grade I tumors and 28 grade 1.5 tumors with no radiation history. Of the 28 grade 1.5 meningiomas, 16 were obtained from the 1^{st} operation and 12 from the 2^{nd}-5^{th} operation. To address whether RB1 S780 staining occurs prior to the recurrence or progression, we have separated out the samples obtained at the 1^{st} and subsequent

(2^{nd}-5^{th}) operations, for clarity (see Supplementary Tables S9 and S10). The Figure 3l shows a KM curve comparing three groups (without prior radiation): grade I, grade 1.5 at 1^{st} operation and grade 1.5 at 2^{nd}-5^{th} operation. Phosphorylated RB1 S780, identifies the grade 1.5 group regardless of timing of tissue collection (Figure 3l). The difference in progression free survival, between grade 1.5 groups (1^{st} vs. subsequent operations), was not significant (p=0.236). To further illustrate the specificity of phosphorylated Rb1 S780 for the grade 1.5 group of tumors, an analysis was undertaken in grade 2 and 3 meningiomas. Rb1 S780 staining in histologically aggressive meningiomas (grade II + III), without prior radiation, did not correlate with progression/recurrence-free survival (Figure 3m). Rb1 staining at the S780 site is a unique, specific and robust marker for grade 1.5 meningiomas and may highlight a pathway that can be exploited for therapies.

Screening of the *SMO*, *KLF4*, *TRAF7*, *NF2*, and *AKT* E17K mutations by MIP and relationship with RB1 S780 staining.

Recurrent mutations in *SMO*, *KLF4*, *TRAF7*, *NF2*, and *AKT* genes (31), could potentially underlie the pathogenesis of grade 1.5 meningiomas. We sought to explore the relationship between alterations in these genes and both RB1 S780 staining and recurrence/progression free survival. Target resequencing of *NF2, TRAF7*, *SMO*, *KLF4*, and *AKT1* E17K was performed in an additional cohort of 79 tumors (26 grade I, 25 grade 1.5, 26 grade II and 2 grade III) with both MIP genotyping and RB1 S780 staining. The Tables 2a and 2b show the analyses for testing a relationship between WHO grade and presence of mutation for each of 6 genetic factors, as well as RB1 S780 staining, respectively. Exact logistic regression was used in order to avoid the pitfalls of low cell counts, thus correlated effects due to repeated subjects were ignored. The only mutation showing a significant relationship with grade is TRAF7, which remained statistically significant (p=.020) after adjusting for the experiment-wise error due to multiple comparisons (Holm-Bonferroni, m=6). However, the strength of this relationship appears to be driven mainly by the high prevalence in Grade I as compared to Grades 1.5/II/III. There are no discernable differences in prevalence or odds-ratios among the higher grades, thus inferring a monotonic relationship among the higher grades is not necessarily warranted. Mutations in SMO initially showed significance on its own, but the effect (which was in the opposite direction of TRAF7) washed away after adjusting for multiple comparisons (p=.108). High RB1 was highly related to grade in the mutation (N=79, p=.008) and non-radiated (N=107, p=.013) samples, but less so in the full

(N=140, p=.059) sample. However, note that the relationship is decidedly not monotonic, as contrary to the mutation analyses the odds ratios decrease within just the higher grades (1.5/II/III). For this reason, the relationship would be better characterized with grade as dichotomous (i.e. I vs 1.5/II/III). RB1 S780 staining was most reliable in identifying the grade 1.5 meningiomas, in this group.

We next aimed to test for a relationship between recurrence/progression time and presence of mutation for each of 6 genetic factors. The Supplementary Table S12 summarizes the difference between each of the "no-mutation" and "mutation" survival curves (log-rank test), and also provides estimates of hazard ratios and mean time to recurrence (Cox proportional-hazards regression). Presence of the TRAF7 mutation was associated with lower risk for recurrence/progression (Hazard Ratio = 0.18, 95% CI = 0.04, 0.77, p=.009), even after adjustment for multiple comparisons (p=.044). Presence of the KLF4 mutation was associated with higher risk for recurrence/progression (Hazard Ratio = 9.65, 95% CI = 2.12, 43.9, p<.001), even after adjustment for multiple comparisons (p=.002). The KLF4 and SMO hazard-ratio estimates should be considered unreliable due to the low prevalence of mutation. While TRAF7 and KLF4 mutations may correlate with decreased and increased risk of recurrence/progression, respectively, neither alteration identified the grade 1.5 meningiomas. RB1 S780 staining was most reliable in identifying the grade 1.5 meningiomas with a decrease in progression free survival.

Discussion

Meningiomas are a heterogeneous group of tumors, characterized by WHO grading. Up to 20% of benign meningiomas reoccur even after gross resection (6) and progression of residual disease can be rapid (7). Radiation or radiosurgery are usually reserved for when surgery is not an option, although some tumors prove refractory to this treatment (8). These observations support the concept of a group of histologically benign meningiomas, which clinically behave more aggressively. Identifying these outliers is imperative for treatment planning and surveillance, prior to clinical aggressiveness. When WHO I meningiomas invade brain, they are automatically upgraded to WHO II (2). This diagnosis is dependent on the presence of brain tissue in the histological specimen, bringing up the possibility of WHO I tumors being under graded because of the lack of brain tissue in the specimen. Since these tumors follow a different natural history and recurrence pattern, it is imperative to identify them. These tumors have similar MIB, ki67 and histology patterns (4). Improved biomarkers for identification of these outlying tumors would aid in better classifying for adjuvant planning.

Numerous studies have focused on DNA alterations in aggressive meningiomas (35, 36). Chromosomal gains and losses (37), (e.g. monosomy 22) or specific genotypes (e.g. *NF2* mutations) and next-generation sequencing (31), are promising. The majority of WHO grade I meningiomas (50%–60%) are linked to *NF2* mutations. We performed target resequencing of *NF2, TRAF7*, *SMO*, *KLF4*, and *AKT1* E17K in an additional cohort of meningioma samples, including the discovery set samples (Supplementary Table S3 and S4). The Table 2a shows the analysis testing for a relationship between grade and presence of mutation for each of 6 genetic factors (5 gene mutations and Wild-type). We did not find a correlation between alterations in *SMO*, *KLF4*, *TRAF7*, *NF2*, and *AKT* E17K mutations with WHO grade or clinical aggressiveness of grade 1.5 tumors. There was a trend of TRAF7 mutations and more benign natural history. Further, there was a trend of KLF4 mutations and a more rapid recurrence/progression natural history. While these results must be confirmed in a much larger cohort of samples with excellent clinical outcome data, it is even more impressive that Rb1 S780 staining performed well in identifying grade 1.5 tumors in this group of samples.

Gene expression profiling focused on tumor grade specific transcription has been useful for showing unique profiles. A recent study shed light onto several meningioma subgroups, defined by genome methylation status, including an aggressive subgroup of

WHO grade I tumors (13). Utilizing 2D gel electrophoresis and MS, our group detected a unique group of proteins that distinguished clinically aggressive grade I tumors (10). Focusing on phosphorylation events, AKAP12 was also associated with meningioma progression (16). Proteomic studies can add to the increasing volume of genetic and transcriptional studies, toward a goal of better biomarkers for meningioma patients. These data provide proof of this concept.

In the classification of gliomas, the use of FISH for detection of 1p/19q loss in oligodendrogliomas directs therapy and predicts natural history (38). Further, MGMT hypermethylation and IDH1 mutation status help with prognosticating in high-grade gliomas (39). These examples provide real time biomarkers shedding light onto the pathogenesis of a solid brain tumor, where WHO grading is insufficient.

Protein modulation is an end result of changes in genetic variants, epigenetic alterations and gene transcription. Study of an aggressive tumor's proteome has been instrumental in the identification of targets for therapeutic strategies. Emerging proteomic techniques have shown potential to characterize the dynamic regulation or dysregulation of protein expression and function. Cancer proteomic profiling has been used for the characterization of specific tumors and systematic review of these data using bioinformatics has provided insight into pathophysiology.

Kinase inhibitors have played an important role in the treatment of cancer, thus we utilized proteomic techniques focusing on phosphorylation events. Our group assessed iTRAQ phosphoproteome and kinome peptide array profiling in WHO grade II and III meningiomas (16). This study was validated in a larger cohort of patients and clearly illustrates how analysis of protein functions and networks can yield unique signature and targets of potential diagnostic and prognostic value, in well-defined histological specimens (16).

Using a similar experimental design (16), we identified dysregulated proteins and cascades in clinically aggressive 1.5 meningiomas. While unique and well-defined signatures were seen across meningioma grades (16), dramatic molecular differences were not observed between WHO I versus 1.5. These observations were not unexpected with both having WHO I bland histological features. iTRAQ and peptide chip identified 32 phosphoproteins and 10 phosphopeptides, respectively. Combined datasets revealed mechanisms of 1.5 tumors, allowing molecular characterization. AKT mutation or activation is not a defining feature of this group. The AHR cascade can affect cellular transduction through interactions with Rb (40).

Evidence for Rb1 signaling in the pathogenesis of grade 1.5 meningiomas is as follows: 1. the kinome revealed a significant increase in Rb1 phosphorylation levels predicted to occur at the S780 site, 2. the predicted phosphorylation site is a consensus for CDKs kinases, 3. the canonical pathway analysis identified the cell cycle G1/S checkpoint signaling and western blot analysis revealed significant related increases in CDK4, CDK6 and Rb1 S780 (Figure 2e). Rb1 is a commonly affected tumor suppressor gene in cancers (41), regulating multiple pathways to influence proliferation, migration, invasion, and cell cycle (42). Identification of hyperphosphorylation on RB_774_78 in grade 1.5 meningiomas defined this group. Phosphorylation of many sites on Rb1 by the cyclins/CDKs has been described (43, 44). Rb1 harbors up to 16 potential S/T-P consensus sites for CDKs (44). The majority of the phosphosites are clustered at the carboxyl-terminus. The RB_774_786 (T-R-P-P-T-L-S-P-I-P-H-I-P) peptide contains 3 phosphosites: T774, T778, and S780. The sequence of RB_774_786 (T-R-P-P-T-L-S-P-I-P-H-I-P) displays the S/T-P consensus site, which includes T778 and S780. The consensus analysis predicted S780 as being the most likely to be phosphorylated (score = 0.926) when compared to T774 and T778 sites (Supplementary Figure S3c). Rb1 S780 has been described (45) while T774 and T778 remain uncharacterized. A commercially available antibody allowed investigation of S780 hyperphosphorylation. Our results demonstrate that inactivation of Rb1/EF2 signaling can distinguish the subgroup of 1.5 meningioma from WHO I. The kinome profiling suggested mTOR phosphorylation (FRAP_2443_2455) is upregulated in 1.5 meningiomas (Fig 1c, Supplementary Table S7). The literature reports that Rb1 pathway inactivation results in mTOR overexpression (46). mTOR may directly regulate AKT phosphorylation, by decreasing AKT S473 (Fig 4a) aiding mTORC1 upregulation (47) (Fig 4). While our data reveal a decrease in both AKT S473 and T308 and no change in RPS6KB1 T389, the relationship to mTOR is unsettled (Figure 2a). This will be the focus of future work. The increase in Rb1 S780 phosphorylation may be driven by CDK4/6 overexpression (Figure 2e and Figure 4) which results in the dissociation of E2F-1, allowing E2F-1 to activate the transcription of genes required for DNA synthesis and cell cycle progression (45).

Phosphorylation of Rb1 S780 proved to be a real time biomarker for identifying the 1.5 meningiomas. Hyperphosphorylation of Rb1 S780 correlated with increased recurrence/progression in a comprehensive cohort of patients. This was not the case in WHO grade I, II or III tumors, illustrating the specificity for grade 1.5 meningiomas.

While all grade I tumors, in the discovery set, were first time surgery samples, 3/5 of the grade 1.5 tumors were initial surgical samples. None of the discovery set samples had been treated with radiation prior to surgery. To understand if Rb1 S780 is predictive we organized a TMA cohort of samples including WHO grade I, 1.5, II and III meningiomas. Samples were from initial and subsequent (2^{nd}-5^{th} operations) interventions and sometimes before or after radiation treatments. RB1 S780 staining was specific for the grade 1.5 group of meningiomas. Patterns for high Rb1 S780 staining: at the 1^{st} surgery, or 2^{nd} through 5^{th} remained high. This suggests that Rb1 S780 is phosphorylated at an early stage when WHO grade I histology is reflected, predicting the clinical activity seen with these aggressive tumors. Rb1 staining did not have this predictive ability in post-radiation cases. Rb1 dephosphorylation upon radiation treatment occurs (34) and may be involved with meningioma escape from treatment. It is very interesting that the levels of RB1 S780 staining are also decreased (to levels seen in WHO grade I tumors) in the more aggressive WHO grade II and III tumors, before and after radiation. This likely reflects the complexity and heterogeneous nature of meningiomas, deeper than the WHO grading scheme. The potential for therapeutic targeting of the RB1 pathway may lead to better outcomes for this particular subset of grade 1.5 tumors. To this end, the *in vitro* characterization of the Rb S780 site is under investigation.

Other authors have identified this group of histologically benign meningioma with clinically aggressive behavior (3, 4, 5, 6, 8, 12). So far, proposed molecular grading schemes for 1.5 meningioma have been based mainly on cytogenetics. The identification of chromosomal abnormalities (12, 6) with potential prognostic value have been reported in histologically benign meningiomas. A recent study shed light onto several meningioma subgroups defined by genomic methylation status (13). Compared with WHO grading, classification by individual and combined methylation classes more accurately identifies patients at high risk of disease progression in tumors with WHO I histology (13). While mutational analysis and genome methylation are promising, our data demonstrate the potential of Rb1 S780 staining for the diagnosis of 1.5 meningiomas and a marker for recurrence. Non-irradiated grade 1.5 samples had significant hyperphosphorylation at RB1 S780, versus WHO I. In resequencing NF2, SMO, AKT, KLF4 and TRAF7 we found that mutations did not correlate with RB1 S780 staining. While there may be trends for TRAF7 and KLF4 mutations in benign and aggressive courses, respectively, these alterations did not identify grade 1.5

meningiomas. Mechanisms driving the clinical phenotype and oncogenesis of meningiomas are very complicated. Prognostic biomarkers and treatments are likely to draw from genetic, transcriptional, epigenetic and proteomic mechanisms. The time has come for meningioma pathologic specimens to be analyzed with several biomarkers for the most accurate identification and prediction of clinical course. This will result in the best outcomes for meningioma patients.

Taken together, these data provide a basis for the concept that Rb1 S780 phosphorylation may play a role in the progression/recurrence phenotype in grade 1.5 meningiomas, and suggest it may be a potential predictive biomarker. Staining of Rb1 S780 is a promising biomarker for risk stratification, diagnosis, and should be validated in a larger prospective cohort.

References

1. Wiemels J, Wrensch M, Claus EB. Epidemiology and etiology of meningioma. J Neurooncol 2010;**99**:307–14.
2. Louis DN, Perry A, Reifenberger G, von Deimling A, Figarella-Branger D, et al. The 2016 World Health Organization Classification of Tumors of the Central Nervous System: a summary. Acta Neuropathol2016;**131**:803-20.
3. Pramesh CS, Saklani AP, Pantvaidya GH, Heroor AA, Naresh KN, et al. Benign metastasizing meningioma. Jpn J Clin Oncol 2003;**33**:86-8.
4. Nakasu S, Fukami T, Jito J, Nozaki K. Recurrence and regrowth of benign meningiomas. Brain Tumor Pathol 2009;**26**:69-2.
5. Kotapka MJ, Kalia KK, Martinez AJ, Sekhar LN. Infiltration of the carotid artery by cavernous sinus meningioma. J Neurosurg 1994;**81**:252–55.
6. Kakkar A, Kumar A, Das A, Pathak P, Sharma MC, et al. 1p/14q co-deletion: A determinant of recurrence in histologically benign meningiomas. Indian J Pathol Microbiol 2015;**58**:433-38.
7. Marciscano AE, Stemmer-Rachamimov AO, Niemierko A, Larvie M, Curry WT, et al. Benign meningiomas (WHO Grade I) with atypical histological features: correlation of histopathological features with clinical outcomes. J Neurosurg 2015;**14**:1-9.
8. Pollock BE, Stafford SL, Link MJ, Garces YI, Foote RL. Single-fraction radiosurgery of benign cavernous sinus meningiomas. J Neurosurg 2013;**119**:675-82, 2013.
9. Perry A, Scheithauer BW, Stafford SL, Lohse CM, Wollan PC. "Malignancy" in meningiomas: a clinicopathologic study of 116 patients, with grading implications. Cancer 1999;**85**:2046-56.
10. Osbun, J, Tatman PD, Kaur S, Parada CA, Busald T., et al. Comparative Proteomic Profiling Using Two- Dimensional Gel Electrophoresis and Identification via LC-MS/MS Reveals Novel Protein Biomarkers to Identify Aggressive Subtypes of WHO Grade I Meningioma. J. Neurol. Surg 2017;**78**:371-79.
11. Kumar S, Kakkar A, Suri V, Kumar A, Bhagat U, et al. Evaluation of 1p and 14q status, MIB-1 labeling index and progesterone receptor immunoexpression in meningiomas: Adjuncts to histopathological grading and predictors of aggressive behavior. Neurol India 2014;**62**:376-82.

12. Barbera S, San Miguel T, Gil-Benso R, Muñoz-Hidalgo L, Roldan P, et al. Genetic changes with prognostic value in histologically benign meningiomas. Clin Neuropathol 2013;**32:**311-17.
13. Sahm F, Schrimpf D, Stichel D, Jones DTW, Hielscher T, et al. DNA methylation-based classification and grading system for meningioma: a multicentre, retrospective analysis. Lancet Oncol 2017;**18**:682-94.
14. Ostasiewicz P, Zielinska DF, Mann M, Wiśniewski JR. Proteome, phosphoproteome, and N-glycoproteome are quantitatively preserved in formalin-fixed paraffin-embedded tissue and analyzable by high-resolution mass spectrometry. J Proteome Res 2010;**9**:3688-700.
15. Pan C, Olsen JV, Daub H, Mann M. Global effects of kinase inhibitors on signaling networks revealed by quantitative phosphoproteomics. Mol Cell Proteomics 2009;**8**:2796-808.
16. Parada CA, Kaur S, Tatman P, Shi M, Busald T, et al. Phosphoproteomic signature of aggressive meningiomas reveals the A kinase (PRKA) anchor protein (gravin) 12 as a central regulator of migration, invasion, and cell cycle in meningioma malignancy. Sci Rep 2018;**8**:2098.
17. Gulmann C, Sheehan KM, Conroy RM, Wulfkuhle JD, Espina V, et al. Quantitative cell signaling analysis reveals down-regulation of MAPK pathway activation in colorectal cancer. J Pathol 2009;**218**:514-19.
18. Gembitsky DS, Lawlor K, Jacovina A, Yaneva M, Tempst P. A prototype antibody microarray platform to monitor changes in protein tyrosine phosphorylation. Mol Cell Proteomics 2004;**3**:1102-18.
19. Guo L, Xiao Y, Fan M, Li JJ, Wang Y. Profiling global kinome signatures of the radioresistant MCF-7/C6 breast cancer cells using MRM-based targeted proteomics. J Proteome Res 2015;**14**:193-01.
20. Klammer M, Kaminski M, Zedler A, Oppermann F, Blencke S, et al. Phosphosignature predicts dasatinib response in non-small cell lung cancer. Mol Cell Proteomics 2012;**11**:651-58.
21. Wibom C, Mörén L, Aarhus M, Knappskog PM, Lund-Johansen M, et al. Proteomic profiles differ between bone invasive and noninvasive benign meningiomas of fibrous and meningothelial subtype. J Neurooncol 2009;**94**:321-01.

22. Barkhoudarian G, Whitelegge JP, Kelly DF, Simonian M. Proteomics Analysis of Brain Meningiomas in Pursuit of Novel Biomarkers of the Aggressive Behavior. J Proteomics Bioinform 2016;**9**:53-7.
23. Abdi F, Quinn JF, Jankovi J, McIntosh M, Leverenz JB, et al. Detection of biomarkers with a multiplex quantitative proteomic platform in cerebrospinal fluid of patients with neurodegenerative disorders. J Alzheimers Dis 2006;**9**,293-48.
24. Shi M, Bradner J, Bammler TK, Eaton DL, Zhang J, et al. Identification of glutathione S-transferase pi as a protein involved in Parkinson disease progression. Am J Pathol 2009;**175**:54-5.
25. Lin X, Shi M, Masilamoni JG, Dator R, Movius J, et al. Proteomic profiling in MPTP monkey model for early Parkinson disease biomarker discovery. Biochim Biophys Acta 2015;**1854**:779-87.
26. Datta, A, Qian J, Chong R, Kalaria RN, Francis P, et al. Novel pathophysiological markers are revealed by iTRAQ-based quantitative clinical proteomics approach in vascular dementia. J Proteomics 2014;**99**:54-7.
27. Datta, A, Chai YL, Tan JM, Lee JH, Francis PT, et al. An iTRAQ-based proteomic analysis reveals dysregulation of neocortical synaptopodin in Lewy body dementias. Mol Brain 2017;**10:**36.
28. Xue Y, Liu Z, Cao J, Ma Q, Gao X, et al. GPS 2.1: enhanced prediction of kinase-specific phosphorylation sites with an algorithm of motif length selection. Protein Eng Des 2011;**24**:255-00.
29. Chartier M., Chenard T, Barker J, Najmanovich, R. Kinome Render: a stand-alone and web-accessible tool to annotate the human protein kinome tree. PeerJ 2013;**1**:e126.
30. Blom N, Sicheritz-Ponten T, Gupta R, Gammeltoft S, Brunak S. Prediction of post-translational glycosylation and phosphorylation of proteins from the amino acid sequence. Proteomics 2004;**4**:1633-49.
31. Clark VE, Erson-Omay EZ, Serin A, Yin J, Cotney J, et al. Genomic analysis of non-NF2 meningiomas reveals mutations in TRAF7, KLF4, AKT1, and SMO. Science 2013;**339**:1077-80.
32. Varjosalo M, Keskitalo S, Van Drogen A, Nurkkala H, Vichalkovski A, et al. The protein interaction landscape of the human CMGC kinase group. Cell Rep 2013;**3**:1306-20.

33. Hanks SK and Hunter T. Protein kinases 6. The eukaryotic protein kinase superfamily: kinase (catalytic) domain structure and classification. FASEB J 1995;**9**:576–96.
34. Haapajärvi T, Kivinen L, Pitkänen K, Laiho M. Cell cycle dependent effects of u.v.-radiation on p53 expression and retinoblastoma protein phosphorylation. Oncogene 1995;**11**:151-59.
35. Bi WL, Greenwald NF, Abedalthagafi M, Wala J, Gibson WJ, et al. Genomic landscape of high-grade meningiomas. 2017;**2**:pii:15.
36. Goutagny S, Yang HW, Zucman-Rossi J, Chan J, Dreyfuss JM, et al. Genomic profiling reveals alternative genetic pathways of meningioma malignant progression dependent on the underlying NF2 status. Clin Cancer Res 2010;**16**:4155-64.
37. Lindblom A, Ruttledge M, Collins VP, Nordenskjöld M, Dumanski JP. Chromosomal deletions in anaplastic meningiomas suggest multiple regions outside chromosome 22 as important in tumor progression. Int J Cancer 1994;**56**:354-57.
38. Nigro JM, Takahashi MA, Ginzinger DG, Law M, Passe S, et al. Detection of 1p and 19q Loss in Oligodendroglioma by Quantitative Microsatellite Analysis, a Real-Time Quantitative Polymerase Chain Reaction Assay 2001;**158**:1253–62.
39. Combs ES, Rieken S, Wick W, Abdollahi A, von Deimling A, et al. Prognostic significance of IDH-1 and MGMT in patients with glioblastoma: One step forward, and one step back? Radiat Oncol 2011;**6**:115.
40. Ge NL, Elferink CJ. A direct interaction between the aryl hydrocarbon receptor and retinoblastoma protein. Linking dioxin signaling to the cell cycle. J Biol Chem 1998;**273**:22708–13.
41. Weinberg RA. The retinoblastoma protein and cell cycle control. Cell 1995;**81**: 323–30.
42. Di Fiore R, D'Anneo A, Tesoriere G, Vento R. RB1 in cancer: different mechanisms of RB1 inactivation and alterations of pRb pathway in tumorigenesis. J Cell Physiol 2013;**228**:1676-87.
43. Adams PD. *Regulation of the retinoblastoma tumor suppressor protein by cyclin/cdks.* Biochim Biophys Acta 2001;**1471**:M123–33.
44. Knudsen ES, Wang JY. Differential regulation of retinoblastoma protein function by specific Cdk phosphorylation sites. J Biol Chem 1996;**271**:8313–20.

45. Connell-Crowley L, Harper JW, Goodrich DW. Cyclin D1/Cdk4 regulates retinoblastoma protein-mediated cell cycle arrest by site-specific phosphorylation. Mol Biol Cell 1997;**8**:287-301.
46. El-Naggar S, Liu Y, Dean DC. Mutation of the Rb1 pathway leads to overexpression of mTor, constitutive phosphorylation of Akt on serine 473, resistance to anoikis, and a block in c-Raf activation. Mol Cell Biol. 2009;**29(21)**:5710-17.
47. Breuleux M, Klopfenstein M, Stephan C, Doughty CA, Barys L, et al. Increased AKT S473 phosphorylation after mTORC1 inhibition is rictor dependent and does not predict tumor cell response to PI3K/mTOR inhibition. Mol Cancer Ther 2009;**4**:742-53.

Sample	**Grade**	N (%)	pRB1 Mean	Log pRB1 Mean	Change from Grade I	Change from Grade I (Modelled)	Sig. (vs. Grade I)	Sig. (Ordinal)
Full Sample [1]	Grade I	30 (40%)	0.03	-5.07	---	---	---	.036
	Grade 1.5	15 (20%)	0.11	-2.98	2.09	1.75	.006	
	Grade II	26 (35%)	0.06	-4.41	0.66	0.19	.720	
	Grade III	4 (5%)	0.04	-3.35	1.72	0.88	.410	
No Radiation Tx [2]	Grade I	29 (52%)	0.03	-5.01	---	---	---	.0003
	Grade 1.5	10 (18%)	0.15	-2.00	3.01	3.26	<.0001	
	Grade II	16 (29%)	0.05	-4.60	0.41	0.38	.524	
	Grade III	1 (2%)	0.02	-3.91	1.10	1.11	.566	
Radiation Tx [3]	Grade I	1 (5%)	0.00	-6.63	---	---	---	.911
	Grade 1.5	5 (26%)	0.02	-4.93	1.70	1.20	.526	
	Grade II	10 (53%)	0.09	-4.09	2.54	0.63	.748	
	Grade III	3 (16%)	0.05	-3.16	3.48	0.80	.724	

Table 1a Rb1 S780 phosphorylation by grade.
Statistical significance by mixed-effects regression (log-transformed), using grade ranks to test for an ordinal relationship. [1] Analyses adjust for invasion (p=.06), location on array (p=.02), and sex (p=.29). [2] Analyses adjust for sex (p=.91). [3] Analyses adjust for macronuclei (p=.04) and sex (p=.19)

Figure	Sample	Factor	Significance		Comparison	Hazard Ratio		
			Cox Unadj.	Cox Adjusted		Esti-mate	95% Lower	95% Upper
5f [1]	All	pRb1	.005	.004	pRb1 High (vs. Low)	2.93	1.41	6.09
5g [2]	No Radiation	pRb1	.0002	.0001	pRb1 High (vs. Low)	7.77	2.72	22.2
5h	Radiation	pRb1	.894	---	pRb1 High (vs. Low)	0.90	0.19	4.31
5i [3]	No Radiation	Grade	.066	---	Grade 1.5 (vs. 1)	---	---	---
					Grade 2 (vs. 1)	---	---	---
					Grade 3 (vs. 1)	---	---	---
5j [3]	No Radiation, Grade≤1.5	pRb1	.107	---	pRb1 High (vs. Low)	---	---	---
5k [3]	No Radiation, Grade≥2	pRB1	.934	---	pRb1 High (vs. Low)	---	---	---

Table 1b Rb1 S780 phosphorylation progression/recurrence survival plots.
Some hazard ratios could not be estimated due to low cell counts
[1] Multivariate Cox-model adjusts for grade (p<.01) and small-cell (p=.01)
[2] Multivariate Cox-model adjusts for grade (p=.06), small-cell (p=.01), and sheet architecture (p=.05)
[3] Multivariate Cox-model inconclusive due to low cell counts

	Grade	N (%)	N (%) Mutations	Odds Ratio (vs. I)	Modelled			
					Odds Ratio (vs. I)	Sig. (vs. I)	Sig. Ordinal	Sig. Adj. Multiple Comparisons
NF2	Grade I	26 (33%)	9 (35%)	1.00	1.00	---	.204	.612
	Grade 1.5	25 (32%)	14 (56%)	2.40	2.36	.210		
	Grade II	26 (33%)	14 (54%)	2.20	2.17	.264		
	Grade III	2 (3%)	1 (50%)	1.89	1.84	1.000		
TRAF7	Grade I	26 (33%)	12 (46%)	1.00	1.00	---	.003	.020
	Grade 1.5	25 (32%)	4 (16%)	0.22	0.23	.042		
	Grade II	26 (33%)	3 (12%)	0.15	0.16	.013		
	Grade III	2 (3%)	0 (0%)	0.00	0.53	.635		
AKT1	Grade I	26 (33%)	3 (12%)	1.00	1.00	---	.106	.424
	Grade 1.5	25 (32%)	1 (4%)	0.32	0.33	.640		
	Grade II	26 (33%)	0 (0%)	0.00	0.24	.235		
	Grade III	2 (3%)	0 (0%)	0.00	3.51	1.000		
KLF4	Grade I	26 (33%)	0 (0%)	1.00	1.00	---	.700	1.000
	Grade 1.5	25 (32%)	1 (4%)	---	1.04	.980		
	Grade II	26 (33%)	1 (4%)	---	1.00	1.000		
	Grade III	2 (3%)	0 (0%)	---	---	---		
SMO	Grade I	26 (33%)	0 (0%)	1.00	1.00	---	.022	.108
	Grade 1.5	25 (32%)	1 (4%)	---	1.04	.980		
	Grade II	26 (33%)	5 (19%)	---	7.78	.051		
	Grade III	2 (3%)	0 (0%)	---	---	---		
Wild Type	Grade I	26 (33%)	9 (35%)	1.00	1.00	---	.949	1.000
	Grade 1.5	25 (32%)	7 (28%)	0.73	0.74	.837		
	Grade II	26 (33%)	8 (31%)	0.84	0.84	1.000		
	Grade III	2 (3%)	1 (50%)	1.89	1.84	1.000		

Table 2a Mutation Rate by Grade

Sample	Grade	N (%)	N (%) High	Odds Ratio (vs. I)	Modelled			
					Odds Ratio (vs. I)	**Sig.** (vs. I)	**Sig.** Ordinal	**Sig.** Adj. Multiple Comparisons
N=79 (Table 2A)	Grade I	26 (33%)	5 (19%)	1.00	1.00	---	.001	.008
	Grade 1.5	25 (32%)	24 (96%)	100.80	86.88	<.001		
	Grade II	26 (33%)	19 (83%)	11.40	10.75	<.001		
	Grade III	2 (3%)	0 (0%)	0.00	1.89	1.000		
N=140 (Full Sample)	Grade I	47 (34%)	8 (17%)	1.00	1.00	---	.010	.059
	Grade 1.5	44 (31%)	34 (77%)	16.58	15.89	<.001		
	Grade II	45 (32%)	21 (47%)	4.27	4.20	.004		
	Grade III	4 (3%)	1 (25%)	1.63	1.61	1.000		
N=107 (Full Sample, non-radiated)	Grade I	47 (44%)	8 (17%)	1.00	1.00	---	.002	.013
	Grade 1.5	28 (26%)	27 (96%)	131.63	118.93	<.001		
	Grade II	31 (29%)	15 (48%)	4.57	4.47	.007		
	Grade III	1 (1%)	0 (0%)	0.00	5.00	1.000		

Table 2b Rate of High RB1 by Grade

Odds ratios and statistical significance by exact logistic regression, without adjusting for other factors. Eight subjects are represented twice in this sample, the effects of which this analysis ignores due to the small sample size (which requires exact logistic regression). Adjustment for multiple comparisons by Holm-Bonferroni (m=7)

Figure Legends

Figure 1: Kinome profiling (STK PamChip®) of grade 1.5 meningioma. a: STK PamChip® peptide chip array experimental design and workflow. Grey circle is the theoretical epitope. **b:** Heat map of peptide signal intensities. The bar on the top right shows the relation between 2Log transformed signal intensities and color. Red: hyperphosphorylation. Green: hypophosphorylation. (+) highest phosphorylation levels, (-) lowest phosphorylation levels. Each row represents clustered peptides detected on the STK PamChip® with 2Log signal intensity above the limit of detection (101). Each column represents a group of pooled samples submitted to the kinome profiling (grade I and 1.5). **c:** Fold change analysis (cut-off 20% and p-value<0.05) reveals 10 hyperphosphorylated peptides. RED: upregulation, GREEN: downregulation. The order of phosphorylated peptides is according to fold changes, from largest to smallest. The grey row indicates RB1 chosen for further validation. **d:** The IPA core analysis of hyperphosphorylated peptides in meningioma grade 1.5 predicts activation of Fcγ Receptor-mediated Phagocytosis in Macrophages and Monocytes, Endothelin-1, Type II Diabetes Mellitus, and Glioma signaling pathways. The x-axis shows –log(p-value). The numerical value on the top represents the percentage of genes in the dataset. Numerical values on the right show the number of genes in the canonical pathway.

Figure 2: Western Blotting validation of aggressiveness-related canonical pathways and kinases in grade 1.5 meningioma. Western Blotting assay was performed in three grade I and three grade 1.5 fresh-frozen tissue lysates. Cropped lanes. **a:** PI3K/AKT/MTOR targets. **b:** ERK-MAPK targets. **c:** cAMP/PKA targets. **d:** CDC42-RAC1-RHOA targets. **e:** cell cycle G1/S checkpoint targets. **e:** The table demonstrates a list of significantly altered proteins and kinases in 1.5 meningiomas as well as their respective p-values. Bold letter and ' * ' indicate proteins and kinases with $p < 0.05$. See also Supplementary Figure S7 for band intensity and statistics.

Figure 3: RB1 S780 validation in a TMA cohort of clinical specimens. a: Representative WHO I and 1.5 meningioma H&E section from two cases. **b:** The same representative cases stained with Rb1 S780. Note the increased cytoplasmic and nuclear staining in the 1.5 meningioma. **c**: Ratio of Rb1 S780 staining per total tissue area versus tumor grade – all samples (non-irradiated samples + samples with prior radiation). **d**: Ratio of Rb1 S780 staining per total tissue area versus tumor grade – non-irradiated samples only. **e:** Ratio of Rb1 S780 staining per total tissue area versus tumor grade (only samples with prior radiation). In **c**, **d**, and **e**, x-axis indicates Rb1 S780 intensity of staining. Y-axis shows meningioma grades. "n" indicates number of samples. Statistical significance by mixed-effects regression using grade ranks to test for an ordinal relationship. See also Table 3a and 3b. **f:** Progression/recurrence-free survival versus ratio of Rb1 S780 staining per total tissue area independently of tumor grade – all samples. **g:** Progression/recurrence-free survival versus ratio of Rb1 S780 staining per total tissue area independent of tumor grade in non-irradiated samples. **h:** Progression/recurrence-free survival in irradiated tumors, ratio of Rb1 S780 staining per total tissue area independent of tumor grade. **i:** Progression/recurrence-free survival in all histologically benign meningiomas (grades I: n=47, and 1.5: n=44). **j:** Progression/recurrence-free survival in all non-irradiated histologically benign meningiomas (grades I: n=47, and 1.5: n=28). **k:** Progression/recurrence-free survival in all irradiated histologically benign meningiomas (grades I: n=0, and 1.5: n=16). **l:** Progression/recurrence-free survival in non-irradiated histologically benign meningiomas. Grade I tumors were samples collected at the first and only surgery

(n=47). Grade 1.5 tumors were collected from either initial (1st surgery, n=16) or recurrent (2nd-5th surgery, n=12) specimens. **m:** Progression/recurrence-free survival of grade II and III tumor patients –non-irradiated samples (n=32). Statistical significance by Cox regression. See also Table 3a and 3b.

Figure 4: Proposed meningioma grade 1.5 mechanism of aggressiveness: Gene names are shown at the approximate positions where their encoded proteins function in the pathway. Colored molecules were significantly altered. Grey molecules: affected with no significant changes in regulation. Red molecules: significant upregulation. Green molecules: significant downregulation. Continuous arrows: activation. Dashed arrows: inactivation.

Author Manuscript Published OnlineFirst on October 15, 2019; DOI: 10.1158/1078-0432.CCR-18-0641
Author manuscripts have been peer reviewed and accepted for publication but have not yet been edited.

Fig 1

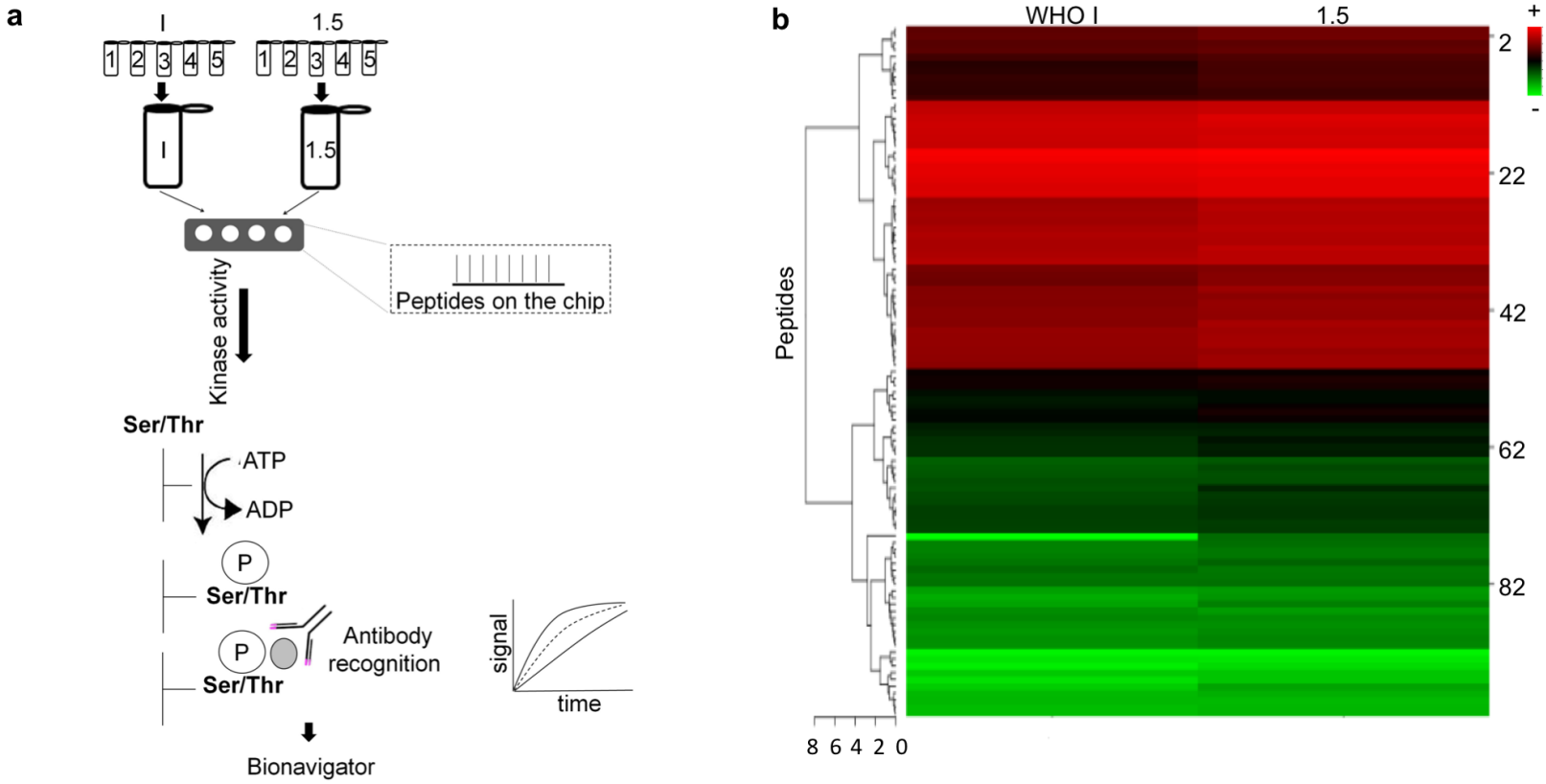

c

Uniprot	Peptide on the Chip	Sequence	Site	1.5 vs I
P06400	RB_774_786	TRPPTLSPIPHIP	T774, T778, S780	3.614
P05771	KPCB_19_31_A25S	RFARKGSLRQKNV	S25	0.823
P42345	FRAP_2443_2455	RTRTDSYSAGQSV	T2444, T2446, S2448, S2450, S2454	0.797
P22001	KCNA3_461_473	GSLCAIAGVLTIA	S462, T471	0.718
P29474	NOS3_1171_1183	SRIRTQSFSLQER	S1171, T1175, S1177, S1179	0.666
P81274	GPSM2_394_406	SSLNGVRPKLGRR	S394, S395	0.641
P14598	NCF1_321_333	QDAYRRNSVRFLQ	S328	0.348
P46020	KPB1_1011_1023	QVEFRRLSISAES	S1018, S1020, S1023	0.326
Na	ART_025	CXGLRRWSLGGLRRWSL	Na	0.288
Q01118	SCN7A_898_910	KNGCRRGSSLGQI	S905, S906	0.213

Downregulated
Upregulated

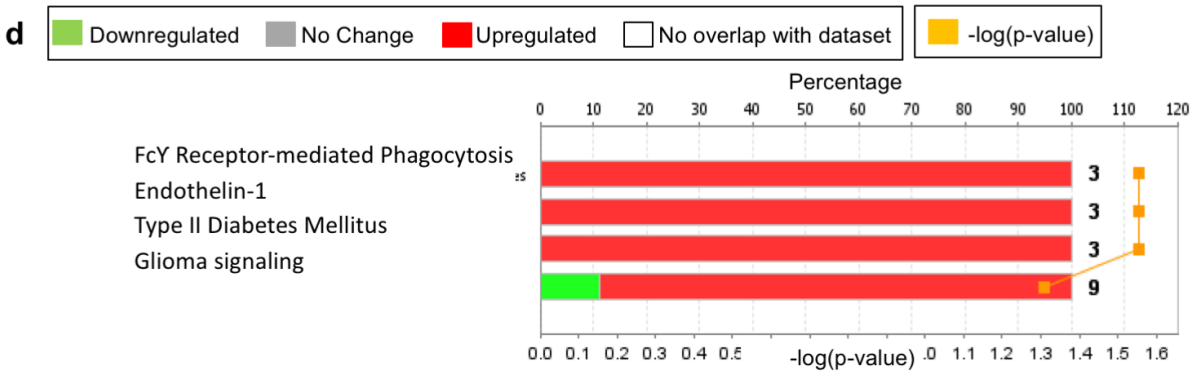

Author Manuscript Published OnlineFirst on October 15, 2019; DOI: 10.1158/1078-0432.CCR-18-0641
Author manuscripts have been peer reviewed and accepted for publication but have not yet been edited.

Fig 2

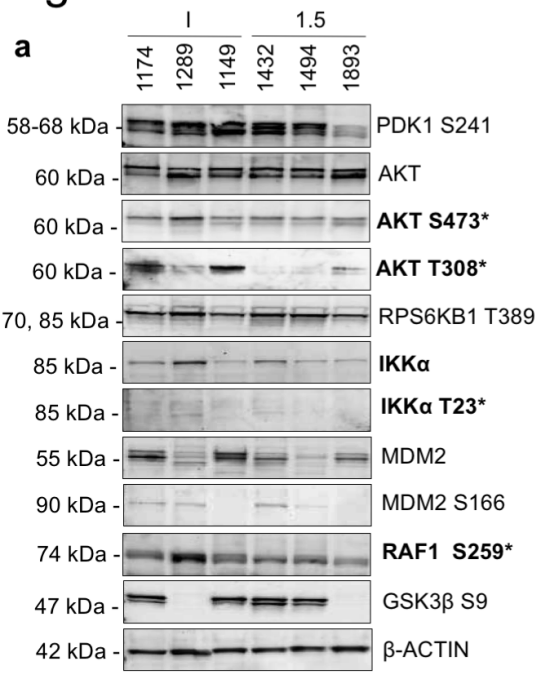

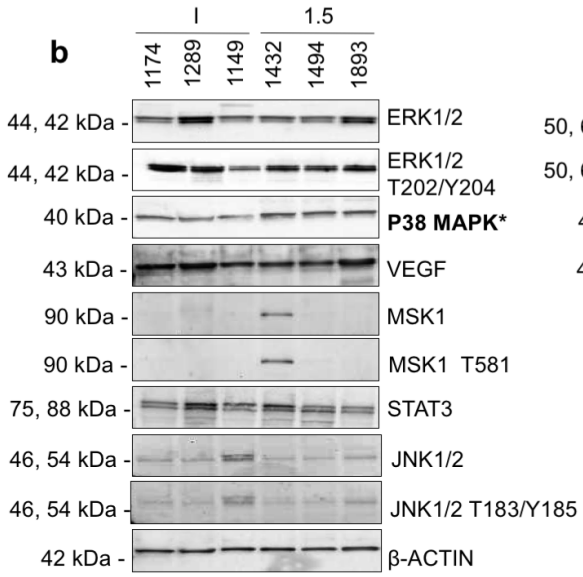

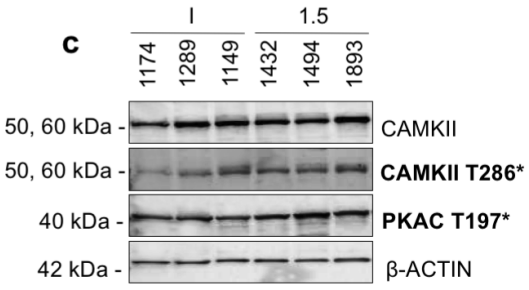

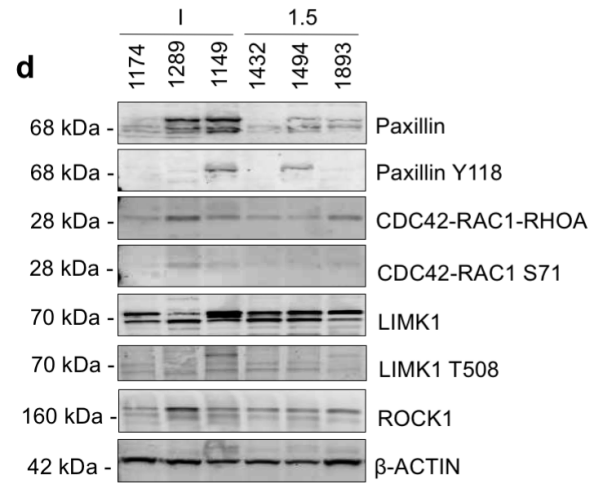

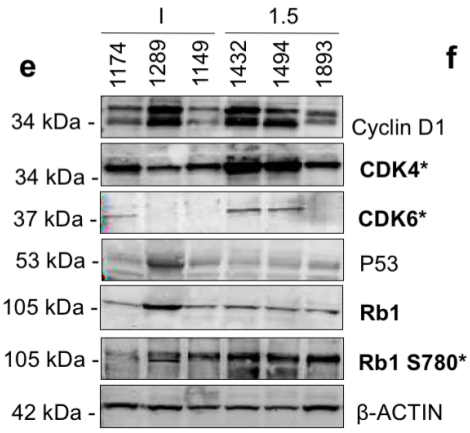

f

Target	p-value	Target	p-value
AKT S473	0.032	CAMKII T286	0.004
AKT T308	0.03	PKAC T197	0.042
IKKα	0.006	CDK4	0.031
RAF1 S259	0.041	CDK6	0.039
p38 MAPK	0.045	Rb1 S780	0.026

Fig 3

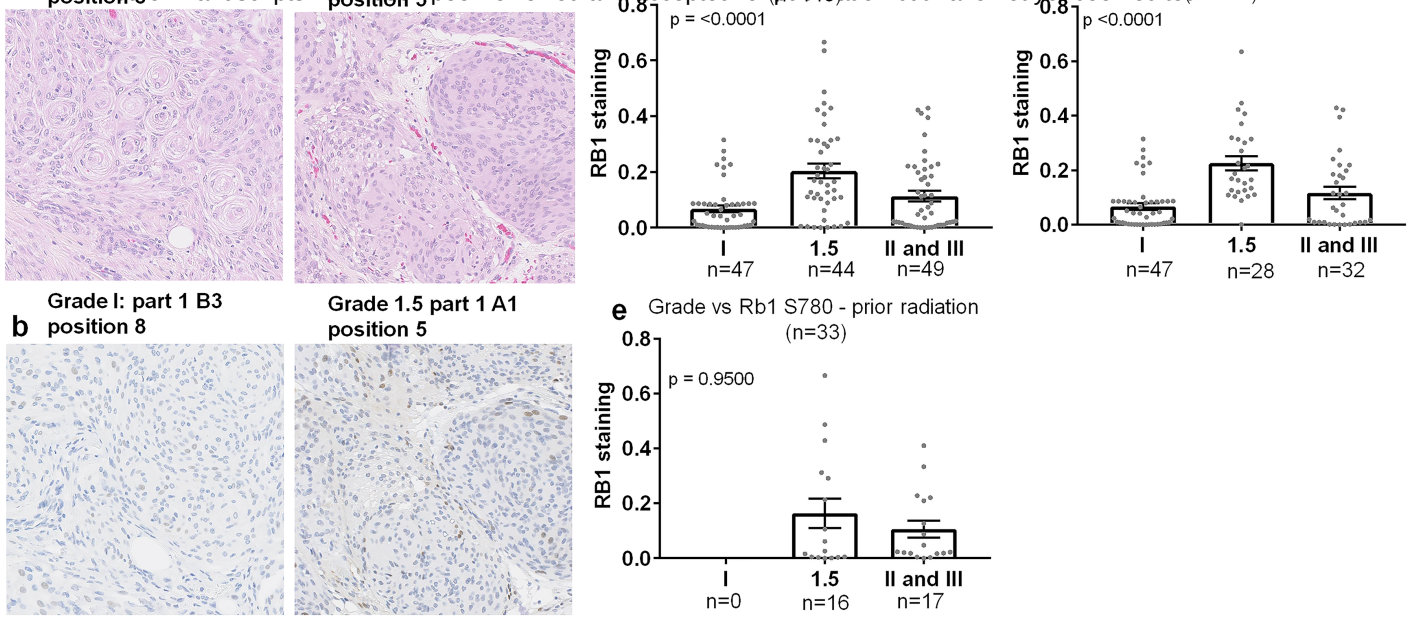

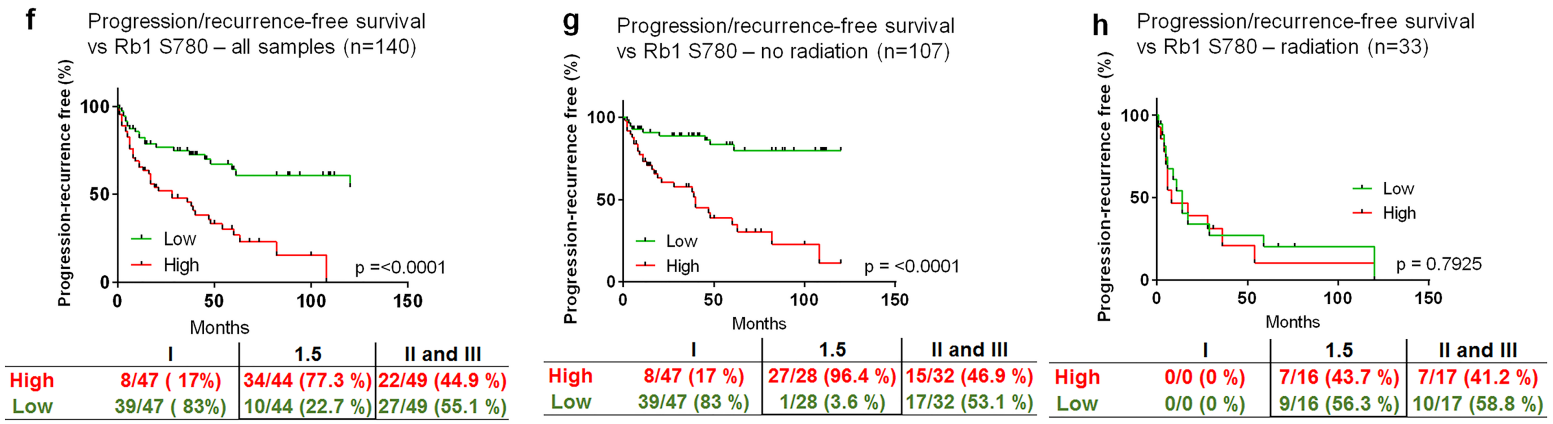

	I	1.5	II and III
High	8/47 (17%)	34/44 (77.3 %)	22/49 (44.9 %)
Low	39/47 (83%)	10/44 (22.7 %)	27/49 (55.1 %)

	I	1.5	II and III
High	8/47 (17 %)	27/28 (96.4 %)	15/32 (46.9 %)
Low	39/47 (83 %)	1/28 (3.6 %)	17/32 (53.1 %)

	I	1.5	II and III
High	0/0 (0 %)	7/16 (43.7 %)	7/17 (41.2 %)
Low	0/0 (0 %)	9/16 (56.3 %)	10/17 (58.8 %)

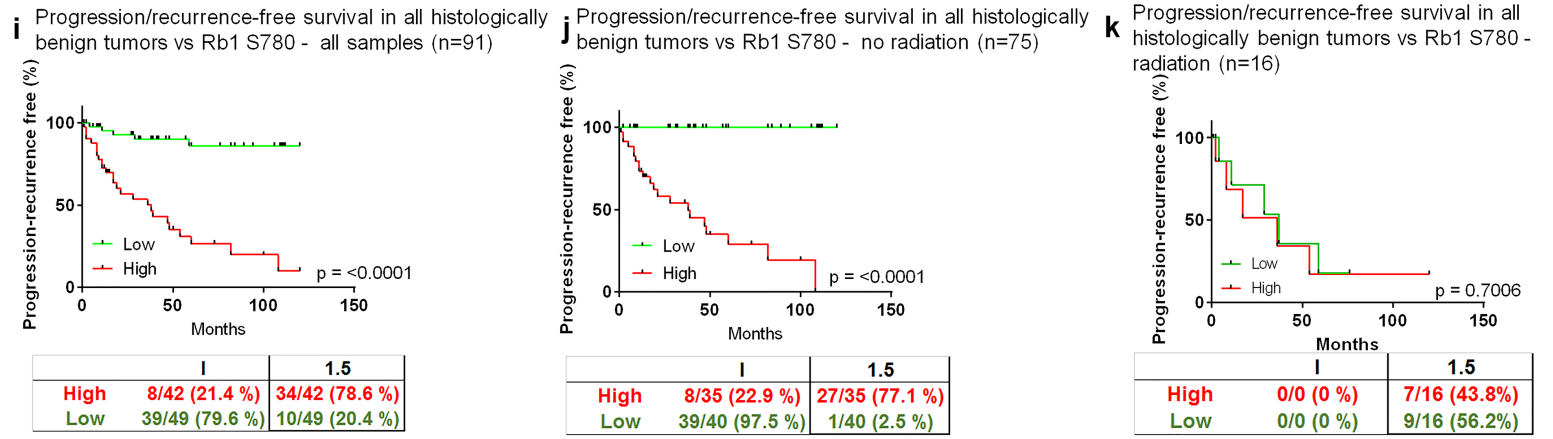

	I	1.5
High	8/42 (21.4 %)	34/42 (78.6 %)
Low	39/49 (79.6 %)	10/49 (20.4 %)

	I	1.5
High	8/35 (22.9 %)	27/35 (77.1 %)
Low	39/40 (97.5 %)	1/40 (2.5 %)

	I	1.5
High	0/0 (0 %)	7/16 (43.8%)
Low	0/0 (0 %)	9/16 (56.2%)

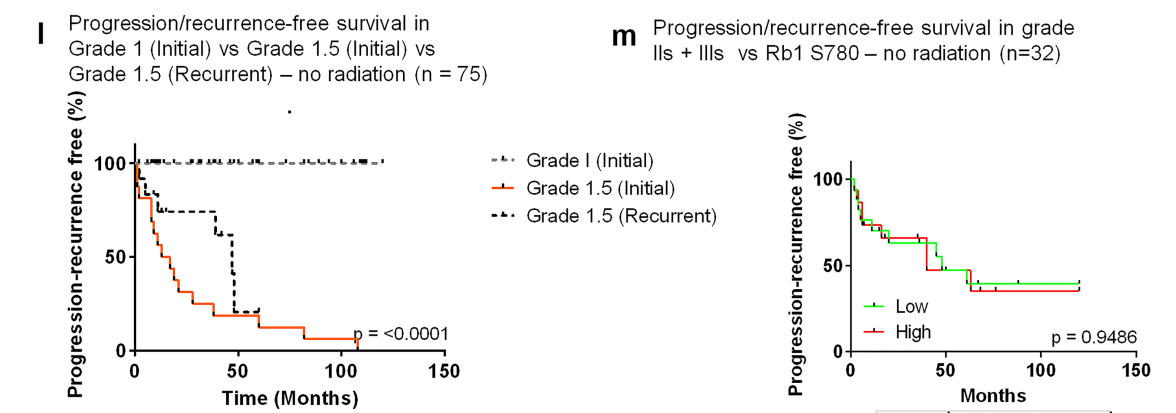

	Grade I	Grade 1.5
Initial	47/47 (100 %)	16/28 (57.1 %)
Recurrent	0 (0 %)	12/28 (42.9%)

	II + IIIs
High	15/32 (46.9 %)
Low	17/32 (53.1 %)

Fig 4

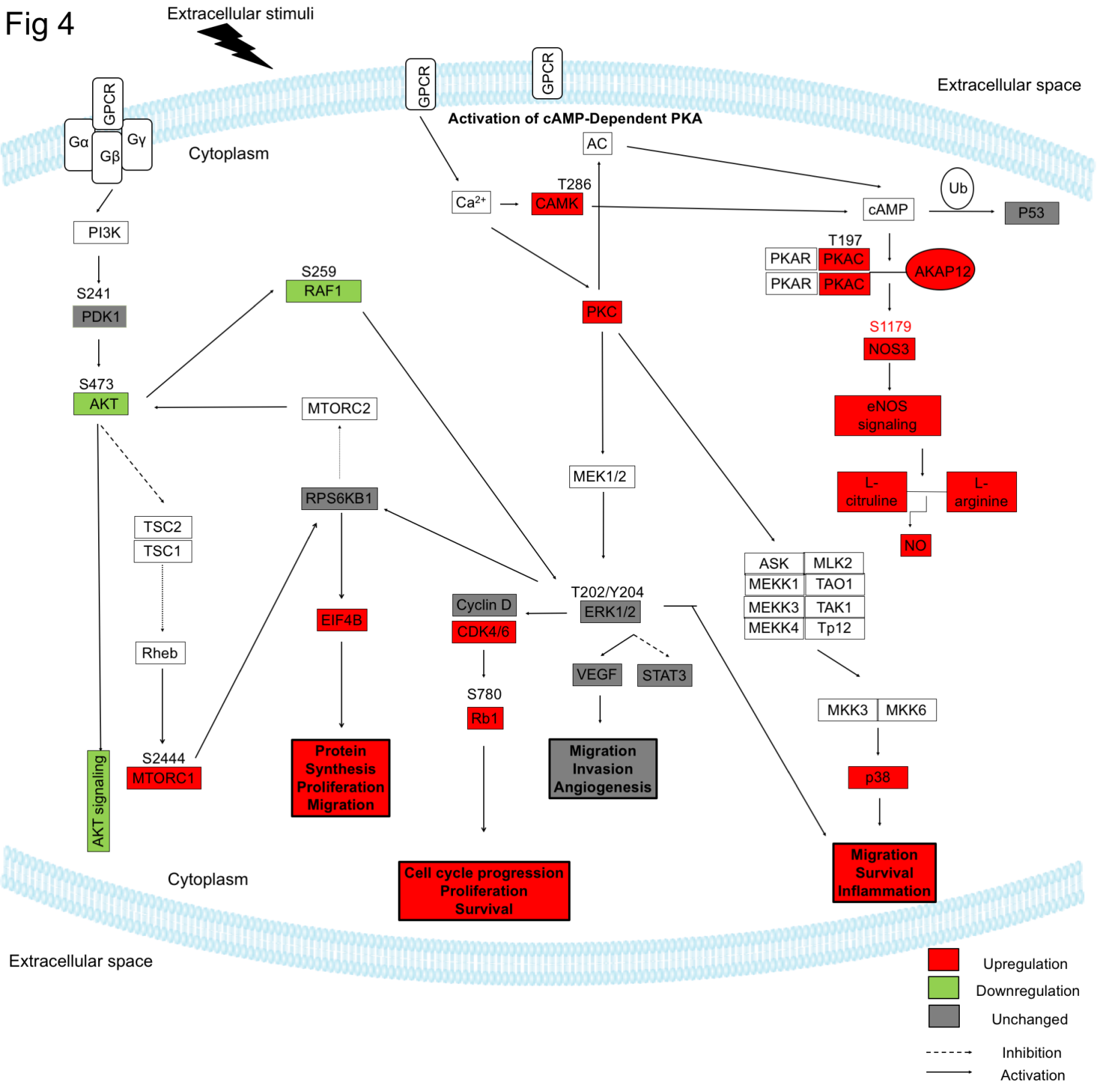

AACR American Association for Cancer Research

Clinical Cancer Research

Phosphoproteomic and Kinomic Signature of Clinically Aggressive Grade I (1.5) Meningiomas Reveals Rb1 signaling as a Novel Mediator and Biomarker

Carolina A Parada, Joshua W Osbun, Tina Busald, et al.

Clin Cancer Res Published OnlineFirst October 15, 2019.